NASA TECHNICAL MEMORANDUM

NASA TM X- 73917

NASA TM X- 73917

(NASA-TM-X-73917) SHOCKLESS AIRFOILS WITH THICKNESSES OF 20.6 AND 20.7 PERCENT CHORD ANALYTICALLY DESIGNED FOR A MACH NUMBER OF 0.68 AND A LIFT COEFFICIENT OF 0.40 (NASA) 38 p HC A03/MF A01 CSCL 01A G3/02

N78-30046

Unclas 29386

SHOCKLESS AIRFOILS WITH THICKNESSES OF 20.6 AND 20.7 PERCENT CHORD ANALYTICALLY DESIGNED FOR A MACH NUMBER OF 0.68 AND A LIFT COEFFICIENT OF 0.40

By Dennis O. Allison

May 76

NASA
National Aeronautics and Space Administration

Langley Research Center
Hampton, Virginia 23665

1. Report No.
NASA TM X-73917

2. Government Accession No.

3. Recipient's Catalog No.

4. Title and Subtitle
Shockless Airfoils With Thicknesses of 20.6 and 20.7 Percent Chord Analytically Designed for a Mach Number of 0.68 and a Lift Coefficient of 0.40

5. Report Date
May 1976

6. Performing Organization Code

7. Author(s)
Dennis O. Allison

8. Performing Organization Report No.

9. Performing Organization Name and Address
NASA Langley Research Center
Hampton, Virginia 23665

10. Work Unit No.
505-06-31-03

11. Contract or Grant No.

12. Sponsoring Agency Name and Address
National Aeronautics and Space Administration
Washington, DC 20546

13. Type of Report and Period Covered
NASA Technical Memorandum

14. Sponsoring Agency Code

15. Supplementary Notes
Special technical information release; not planned for formal NASA publication.

16. Abstract
A 20.8-percent-thick airfoil shape was designed to have shockless inviscid flow at a Mach number of 0.68 and a lift coefficient of 0.40. In order to determine the actual airfoils which would yield this same shockless flow when viscous effects are included, boundary layer displacement thicknesses were subtracted from the "inviscid" shape for Reynolds numbers of 100 and 35 million. This process yielded airfoils with thicknesses of 20.7 and 20.6 percent, respectively. Subtraction of boundary-layer displacement thicknesses for Reynolds numbers below 35 million yielded nonphysical airfoils, that is airfoils with negative thicknesses near the trailing edge. The pitching moment about the quarter-chord point at the design condition was -0.082 for the inviscid shape and, consequently, for both airfoils.

Off-design calculations for the two airfoils were made using a computer program which provides for the interaction of the inviscid-flow and boundary-layer solutions. The pressure distributions of the airfoils were shockless for conditions from the design point to lower Mach numbers and lift coefficients. No boundary-layer separation was predicted except in the last 3-percent chord on the upper surface.

17. Key Words (Suggested by Author(s))
Aerodynamics
Thick Airfoil
Supercritical Airfoil
Transonic
Shockless
Airfoil Design
Hodograph Methoc

19. Security Classif. (of this report)
Unclassified

20. Security Classif. (of this page)
Unclassified

21. No. of Pages
36

22. Price*
$3.75

* For sale by the National Technical Information Service, Springfield, Virginia 22161

SHOCKLESS AIRFOILS WITH THICKNESSES OF 20.6 AND 20.7 PERCENT CHORD ANALYTICALLY DESIGNED FOR A MACH NUMBER OF 0.68 AND A LIFT COEFFICIENT OF 0.40

Dennis O. Allison

Langley Research Center

SUMMARY

A 20.8-percent-thick airfoil shape was designed to have shockless inviscid flow at a Mach number of 0.68 and a lift coefficient of 0.40. In order to determine the actual airfoils which would yield this same shockless flow when viscous effects are included, boundary-layer displacement thicknesses were subtracted from the "inviscid" shape for Reynolds numbers of 100 and 35 million. This process yielded airfoils with thicknesses of 20.7 and 20.6 percent, respectively. Subtraction of boundary-layer displacement thicknesses for Reynolds numbers below 35 million yielded nonphysical airfoils; that is, airfoils with negative thicknesses near the trailing edge. The pitching moment about the quarter-chord point at the design condition was -0.082 for the inviscid shape and, consequently, for both airfoils.

Off-design calculations for the two airfoils were made using a computer program which provides for the interaction of the inviscid-flow and boundary-layer solutions. The pressure distributions of the airfoils were shockless for conditions from the design point to lower Mach numbers and lift coefficients. No boundary-layer separation was predicted except in the last 3-percent chord on the upper surface.

INTRODUCTION

Recent interest in large transport aircraft which carry their cargo in the wing, commonly called span loaders, has stimulated research on airfoils with thicknesses of 20.0-percent chord or more. Shockless or supercritical airfoil sections are particularly advantageous for this application. For a given thickness ratio they will generally yield a higher drag-rise Mach number than more "conventional" sections and their shape is conducive to efficient packaging. A more detailed discussion of the span loader concept is given in reference 1.

The airfoils in the present paper derive from an initial goal of producing an airfoil with a thickness of at least 20.0-percent chord, a lift coefficient of 0.40 and a Mach number near 0.70. A design Mach number of 0.68 was decided on only after considerable effort was expended to push the upper surface separation point as far aft as possible while maintaining attached flow on the lower surface.

A 20.8-percent-thick airfoil shape was designed for shockless inviscid flow at the design Mach number and lift coefficient. In order to determine two actual airfoils which would yield this same shockless flow when viscous effects are included, boundary-layer displacement thicknesses were subtracted from the "inviscid" shape for Reynolds numbers of 100 and 35 million. This process yielded airfoils with thicknesses of 20.7 and 20.6 percent, respectively. Off-design conditions were examined with special attention on wave drag for Mach numbers less than design and increases and decreases in lift at the design Mach number.

SYMBOLS

C_D	drag coefficient
C_ℓ	lift coefficient
C_m	pitching moment coefficient
C_p	pressure coefficient
M_∞	free-stream Mach number
N_R	Reynolds number based on chord
t/c	thickness-to-chord ratio
x/c, y/c	nondimensional coordinates of airfoil

AIRFOIL DESIGN PROCESS

Computer programs for airfoil design and analysis developed by Frances Bauer, Paul Garabedian, David Korn, and Antony Jameson were used in the present work. The design program uses a hodograph method for solving the inviscid full-potential equations (ref. 2). The analysis program uses a finite difference relaxation technique to solve the full-potential equations and includes boundary-layer interaction (ref. 3). In early steps of the design process airfoil shapes for inviscid flow were computed; in subsequent steps, boundary-layer displacement thickness and separation effects were included. At the last step in the process: (1) An airfoil shape for shockless inviscid flow at a given Mach number and lift coefficient was computed, (2) the boundary-layer displacement thicknesses for two Reynolds numbers were computed and subtracted from the inviscid shape to define actual airfoils, and (3) the airfoils were analyzed with boundary-layer interaction at off-design Mach numbers and lift coefficients. Only the results for the last step in the process will be given. The inviscid shape and pressure distribution with the corresponding computer program inputs will be shown first. Next, the airfoils obtained by subtracting the boundary-layer displacement thicknesses for Reynolds numbers of 100 and 35 million will be shown along with selected off-design calculations.

Inviscid Shape at the Design Conditions

An airfoil shape for shockless inviscid flow at the design Mach number and lift coefficient was computed using the design program (ref. 2). The inviscid shape, pressure distribution, and design program inputs are displayed in figure 1 in the pattern of that on pages 107 through 110 of reference 3. (That case in ref. 3 was used as a starting point in the airfoil design process.) The inviscid shape and pressure coefficient distribution (fig. 1(a)), a hodograph plane (fig. 1(b)), tape 6 and tape 7 input parameters (fig. 1(c)), and automation path inputs (fig. 1(d)) are shown. (All input parameters are defined on pages 105 through 108 of ref. 2 and page 289 of ref. 3.) The inviscid shape in figure 1(a) is given in coordinate form in Table I. The designation S(A)INV-0421 is derived from "Shockless," the designer's initials in parenthesis, "Inviscid," and the lift coefficient and thickness.

Two Airfoils at the Design Conditions

One can subtract a boundary-layer displacement thickness from the inviscid shape in Table I to determine an actual airfoil which will have shockless viscous flow at the design Mach number and lift coefficient. This procedure will not work if a boundary layer is so thick that the upper and lower surfaces of an actual airfoil cross near the trailing edge. The trailing edge opening of the inviscid shape was 2.1-percent chord in the present work. Two airfoils were determined: One for N_R = 100 million whose trailing edge thickness was 0.4-percent chord (fig. 2(a)) and another for N_R = 35 million whose trailing edge was closed (fig. 2(b)). For smaller Reynolds numbers the upper and lower surfaces crossed; however, the inviscid shape could be redesigned with a larger trailing-edge opening. Obviously, the inviscid shape in Table I can also be used with displacement thicknesses calculated from other boundary-layer theories.

Coordinates for the airfoils designed for the two Reynolds numbers are given in Tables II and III. The designations S(A)100-0421 and S(A)035-0421 are the same as for the inviscid shape except that the "INV" is replaced by "100" or "035" to indicate the Reynolds number. Viscous effects were computed by the analysis program in which laminar boundary-layer effects were neglected and transition to turbulent boundary layer was set at 14-percent chord which is the location of the upper surface pressure peak (fig. 1(a)). The same transition location was used in the off-design analysis calculations which will be discussed next.

Viscous Airfoil Analysis at Off-Design Conditions

Analysis of airfoil S(A)100-0421 with boundary-layer interaction at N_R = 100 million and off-design Mach numbers and lift coefficients is shown in figures 3 through 5. Results for various Mach numbers at the design lift coefficient (C_ℓ = 0.40) are shown in figure 3. Results at the design Mach number (M_∞ = 0.68) and a lower Mach number (M_∞ = 0.60) are shown in figures 4 and 5, respectively, for various lift coefficients. Note that the drawing at the bottom in figures 3 through 5 is the airfoil plus the boundary layer. Also shown on these figures are any region of supersonic flow, the pressure distribution, the sonic pressure coefficient, the pitching moment coefficient, and the drag coefficient.

Pressure distributions and pitching moments calculated at N_R = 35 million for airfoil S(A)035-0421 were essentially the same as those in figures 3 through 5. Drag coefficients, however, were higher for airfoil S(A)035-0421 than for airfoil S(A)100-0421, analyzed at their design Reynolds numbers. Figure 6 shows C_D versus M_∞ for both airfoils at C_ℓ = 0.40.

CONCLUDING REMARKS

Airfoils with thicknesses of 20.7- and 20.6-percent chord were analytically designed for a Mach number of 0.68, a lift coefficient of 0.40, and Reynolds numbers of 100 and 35 million, respectively. Since these airfoils were obtained by subtracting a boundary layer from an inviscid shape, airfoils for other Reynolds numbers can be obtained by subtracting the appropriate boundary-layer displacement thicknesses. The 100 million Reynolds number airfoil had a trailing-edge thickness of 0.4-percent chord and the 35 million Reynolds number airfoil was closed at the trailing edge.

The two airfoils had essentially the same pressure distributions when analyzed at their design Reynolds numbers for various Mach numbers and lift coefficients. Pressure distributions for the airfoils were shockless from the design point to conditions of lower Mach numbers and lift coefficients. No boundary-layer separation was predicted except in the last 3-percent chord on the upper surface at the design and the off-design conditions for both airfoils.

A large number of changes were required in mathematical input parameters to determine the inviscid shape. Work is being done, however, at Courant Institute of New York University to make the hodograph method of airfoil design easier to use. An improved version of the design program with a velocity distribution input is being formulated.

REFERENCES

1. Whitehead, Allen H., Jr.: Perspective on the Span-Distributed-Load Concept for Application to Large Cargo Aircraft Design. NASA TM X-3320, 1975.
2. Bauer, F.; Garabedian, P.; and Korn, D.: Supercritical Wing Sections. Lecture Notes in Economics and Mathematical Systems, vol. 66, M. Beckmann and H. P. Künzi, eds., Springer-Verlag, 1972.
3. Bauer, F.; Garabedian, P.; Korn, D.; and Jameson, A.: Supercritical Wing Sections II. Lecture Notes in Economics and Mathematical Systems, vol. 108, M. Beckmann and H. P. Künzi, eds., Springer-Verlag, 1975.

TABLE I.- COORDINATES FOR INVISCID SHAPE S(A)INV-0421

(a) Upper surface

x/c	y/c	x/c	y/c
.00000	.00522	.46697	.11703
.00004	.01112	.48554	.11581
.00055	.01706	.50410	.11435
.00153	.02297	.52263	.11267
.00299	.02882	.54111	.11075
.00496	.03455	.55952	.10860
.00745	.04011	.57787	.10621
.01051	.04549	.59612	.10359
.01418	.05065	.61428	.10076
.01849	.05561	.63232	.09771
.02345	.06037	.65024	.09447
.02907	.06494	.66803	.09105
.03535	.06933	.68567	.08746
.04227	.07353	.70315	.08373
.04983	.07754	.72045	.07989
.05804	.08134	.73757	.07595
.06687	.08494	.75447	.07195
.07635	.08832	.77116	.06792
.08647	.09149	.78759	.06389
.09723	.09445	.80376	.05991
.10862	.09723	.81962	.05601
.12063	.09983	.83514	.05223
.13324	.10227	.85028	.04862
.14641	.10455	.86499	.04521
.16012	.10666	.87920	.04204
.17435	.10865	.89285	.03913
.18906	.11046	.90587	.03646
.20422	.11215	.91821	.03409
.21982	.11367	.92981	.03195
.23581	.11504	.94061	.03005
.25218	.11624	.95059	.02837
.26889	.11728	.95971	.02689
.28591	.11816	.96795	.02560
.30322	.11887	.97529	.02448
.32079	.11941	.98172	.02353
.33857	.11978	.98721	.02273
.35656	.11997	.99175	.02208
.37471	.11997	.99532	.02160
.39300	.11978	.99791	.02126
.41140	.11940	.99947	.02107
.42988	.11882	1.00000	.02101
.44841	.11803		

TABLE I.- Concluded.

(b) Lower surface

x/c	y/c
1.00000	0.00000
.99946	.00005
.99783	.00018
.99511	.00035
.99129	.00052
.98639	.00067
.98042	.00077
.97340	.00077
.96535	.00067
.95630	.00042
.94629	.00002
.93534	-.00055
.92350	-.00132
.91079	-.00230
.89728	-.00349
.88298	-.00492
.86797	-.00659
.85227	-.00851
.83596	-.01066
.81907	-.01310
.80167	-.01576
.78381	-.01867
.76555	-.02180
.74695	-.02516
.72807	-.02870
.70896	-.03243
.68968	-.03630
.67029	-.04029
.65084	-.04437
.63138	-.04849
.61197	-.05261
.59263	-.05669
.57341	-.06067
.55432	-.06450
.53540	-.06812
.51662	-.07149
.49800	-.07456
.47951	-.07730
.46113	-.07970
.44285	-.08175
.42466	-.08347
.40654	-.08486
.38852	-.08596
.37061	-.08677
.35283	-.08732
.33519	-.08762
.31773	-.08768
.30047	-.08752
.28345	-.08715
.26668	-.08657
.25020	-.08579
.23404	-.08482
.21823	-.08366
.20280	-.08233
.18776	-.08081
.17316	-.07912
.15901	-.07725
.14534	-.07522
.13217	-.07301
.11953	-.07063
.10743	-.06809
.09586	-.06536
.08492	-.06250
.07454	-.05947
.06478	-.05629
.05564	-.05296
.04714	-.04948
.03929	-.04586
.03211	-.04215
.02563	-.03830
.01987	-.03433
.01486	-.03025
.01066	-.02601
.00727	-.02156
.00466	-.01679
.00272	-.01167
.00132	-.00624
.00043	-.00059
.00000	.00522

TABLE II.- COORDINATES FOR AIRFOIL S(A)100-0421

(a) Upper surface

x/c	y/c	x/c	y/c
0.00000	.00522	.46697	.11633
.00004	.01112	.48554	.11505
.00055	.01706	.50410	.11355
.00153	.02297	.52263	.11181
.00299	.02882	.54111	.10983
.00496	.03455	.55952	.10761
.00745	.04011	.57787	.10515
.01051	.04549	.59612	.10246
.01418	.05065	.61428	.09953
.01849	.05561	.63232	.09639
.02345	.06037	.65024	.09303
.02907	.06494	.66803	.08948
.03535	.06933	.68567	.08575
.04227	.07353	.70315	.08186
.04983	.07754	.72045	.07782
.05804	.08134	.73757	.07367
.06688	.08494	.75447	.06942
.07635	.08832	.77116	.06511
.08647	.09149	.78759	.06077
.09723	.09445	.80376	.05646
.10662	.09722	.81962	.05222
.12063	.09982	.83514	.04813
.13324	.10224	.85028	.04424
.14641	.10450	.86499	.04062
.16012	.10660	.87920	.03729
.17435	.10854	.89285	.03428
.18906	.11033	.90587	.03157
.20422	.11197	.91821	.02915
.21962	.11346	.92981	.02697
.23581	.11479	.94061	.02497
.25218	.11596	.95059	.02306
.26889	.11697	.95971	.02117
.28592	.11782	.96795	.01920
.30322	.11850	.97529	.01714
.32079	.11901	.98172	.01507
.33856	.11934	.98721	.01308
.35656	.11949	.99175	.01116
.37471	.11946	.99532	.00943
.39300	.11924	.99791	.00816
.41140	.11882	.99947	.00742
.42988	.11820	1.00000	.00719
.44841	.11737		

TABLE II.- Concluded.

(b) Lower surface

x/c	y/c	x/c	y/c
0.00000	.00522	.46114	-.07899
.00043	-.00059	.47951	-.07652
.00132	-.00624	.49800	-.07369
.00272	-.01167	.51663	-.07052
.00466	-.01679	.53540	-.06704
.00727	-.02156	.55432	-.06329
.01066	-.02601	.57341	-.05933
.01486	-.03025	.59263	-.05521
.01987	-.03433	.61197	-.05098
.02563	-.03830	.63139	-.04671
.03211	-.04215	.65084	-.04243
.03929	-.04588	.67029	-.03820
.04714	-.04948	.68968	-.03406
.05564	-.05296	.70896	-.03003
.06478	-.05629	.72807	-.02615
.07455	-.05947	.74695	-.02246
.08492	-.06251	.76555	-.01896
.09568	-.06538	.78381	-.01569
.10743	-.06808	.80167	-.01264
.11953	-.07062	.81907	-.00985
.13217	-.07298	.83596	-.00731
.14534	-.07517	.85227	-.00502
.15901	-.07718	.86797	-.00299
.17316	-.07902	.88298	-.00122
.18776	-.08068	.89728	.00031
.20280	-.08216	.91060	.00160
.21823	-.08347	.92350	.00266
.23404	-.08460	.93534	.00350
.25020	-.08554	.94629	.00412
.26668	-.08629	.95630	.00453
.28345	-.08684	.96535	.00475
.30047	-.08719	.97340	.00478
.31773	-.08732	.98042	.00464
.33519	-.08723	.98639	.00438
.35283	-.08690	.99129	.00408
.37061	-.08631	.99511	.00378
.38852	-.08546	.99783	.00346
.40654	-.08433	.99946	.00321
.42[illegible]66	-.08288	1.00000	.00312
.44285	-.08111		

ORIGINAL PAGE IS
OF POOR QUALITY

TABLE III.- COORDINATES FOR AIRFOIL S(A)035-0421

(a) Upper surface

x/c	y/c	x/c	y/c
0.00000	.00522	.46697	.11618
.00004	.01112	.48554	.11490
.00055	.01706	.50410	.11339
.00153	.02297	.52263	.11164
.00299	.02882	.54111	.10965
.00496	.03455	.55952	.10741
.00745	.04011	.57787	.10494
.01051	.04549	.59612	.10222
.01418	.05065	.61428	.09928
.01849	.05561	.63232	.09611
.02345	.06037	.65024	.09272
.02907	.06494	.66803	.08914
.03535	.06933	.68567	.08537
.04227	.07353	.70315	.08142
.04983	.07754	.72045	.07733
.05804	.08134	.73757	.07309
.06688	.08494	.75447	.06873
.07635	.08832	.77116	.06428
.08647	.09149	.78759	.05977
.09723	.09445	.80376	.05525
.10862	.09722	.81962	.05080
.12063	.09981	.83514	.04651
.13324	.10223	.85028	.04246
.14641	.10448	.86499	.03875
.16012	.10657	.87920	.03540
.17435	.10851	.89285	.03242
.18906	.11030	.90587	.02979
.20422	.11193	.91821	.02743
.21982	.11341	.92981	.02529
.23581	.11474	.94061	.02330
.25218	.11590	.95059	.02134
.26889	.11691	.95971	.01936
.28592	.11775	.96795	.01724
.30322	.11842	.97529	.01499
.32079	.11892	.98172	.01273
.33858	.11925	.98721	.01054
.35656	.11939	.99175	.00838
.37471	.11935	.99532	.00641
.39300	.11913	.99791	.00494
.41140	.11870	.99947	.00409
.42988	.11807	1.00000	.00383
.44841	.11724		

TABLE III.- Concluded.

(b) Lower surface

x/c	y/c	x/c	y/c
0.00000	.00522	.46114	-.07885
.00043	-.00059	.47951	-.07636
.00132	-.00624	.49800	-.07351
.00272	-.01167	.51663	-.07031
.00466	-.01679	.53540	-.06681
.00727	-.02156	.55432	-.06303
.01066	-.02601	.57341	-.05903
.01486	-.03025	.59263	-.05487
.01987	-.03433	.61197	-.05061
.02563	-.03830	.63139	-.04630
.03211	-.04215	.65084	-.04198
.03929	-.04588	.67029	-.03771
.04714	-.04948	.68968	-.03353
.05564	-.05296	.70896	-.02946
.06478	-.05629	.72807	-.02555
.07455	-.05947	.74695	-.02182
.08492	-.06251	.76555	-.01828
.09588	-.06538	.78381	-.01497
.10743	-.06808	.80167	-.01190
.11953	-.07062	.81907	-.00907
.13217	-.07297	.83596	-.00650
.14534	-.07515	.85227	-.00419
.15901	-.07716	.86797	-.00213
.17316	-.07899	.88298	-.00033
.18776	-.08064	.89728	.00122
.20280	-.08212	.91080	.00253
.21823	-.08343	.92350	.00361
.23404	-.08455	.93534	.00446
.25020	-.08548	.94629	.00508
.26668	-.08623	.95630	.00549
.28345	-.08677	.96535	.00568
.30047	-.08712	.97340	.00568
.31773	-.08724	.98042	.00549
.33519	-.08714	.98639	.00517
.35283	-.08681	.99129	.00482
.37061	-.08622	.99511	.00447
.38852	-.08536	.99783	.00411
.40654	-.08421	.99946	.00382
.42466	-.08276	1.00000	.00371
.44285	-.08098		

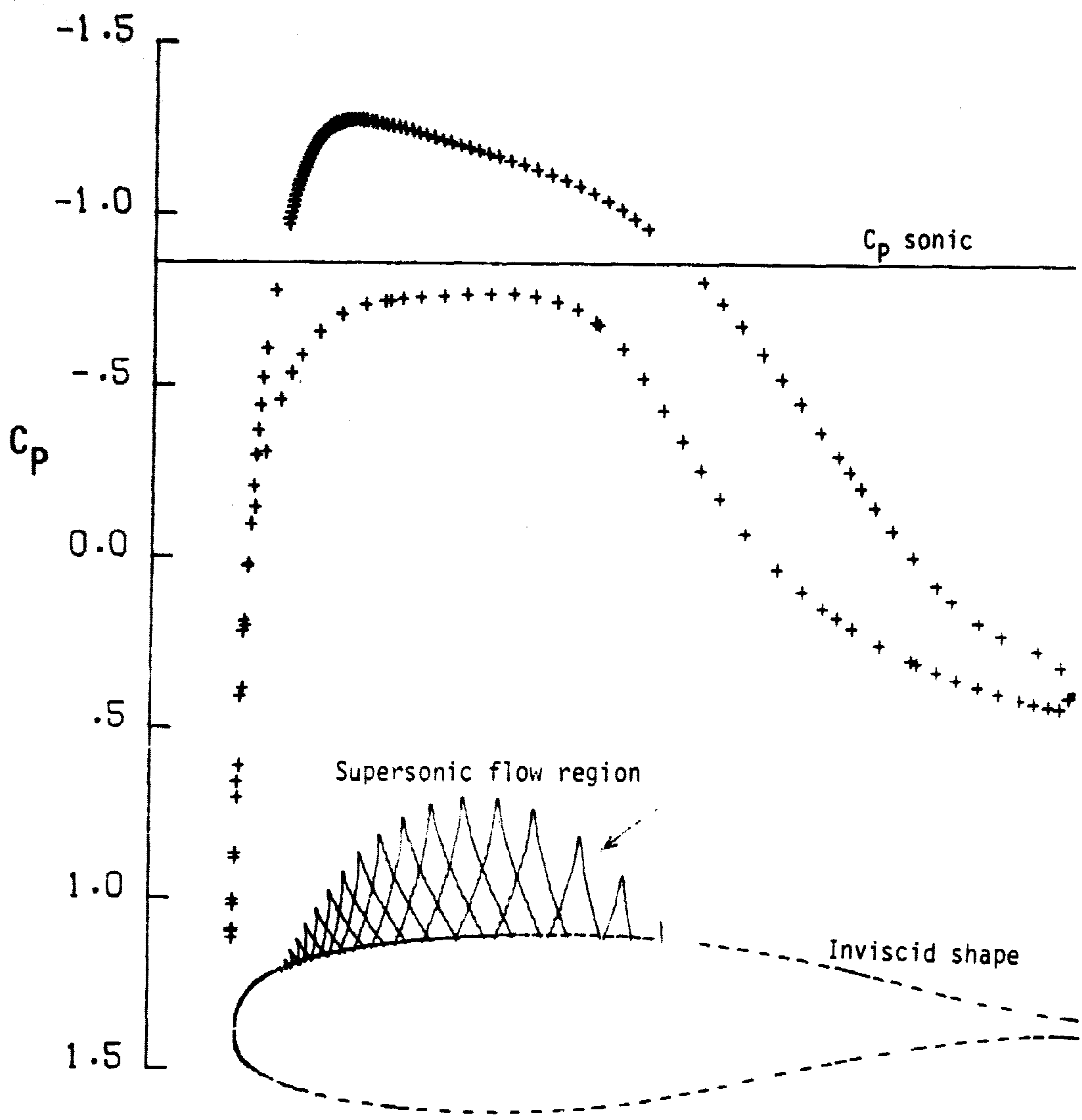

$M_\infty = 0.682$ $C_\ell = 0.400$ $t/c = 0.208$

(a) Inviscid shape and pressure coefficient distribution.

Figure 1.- Hodograph design program output.

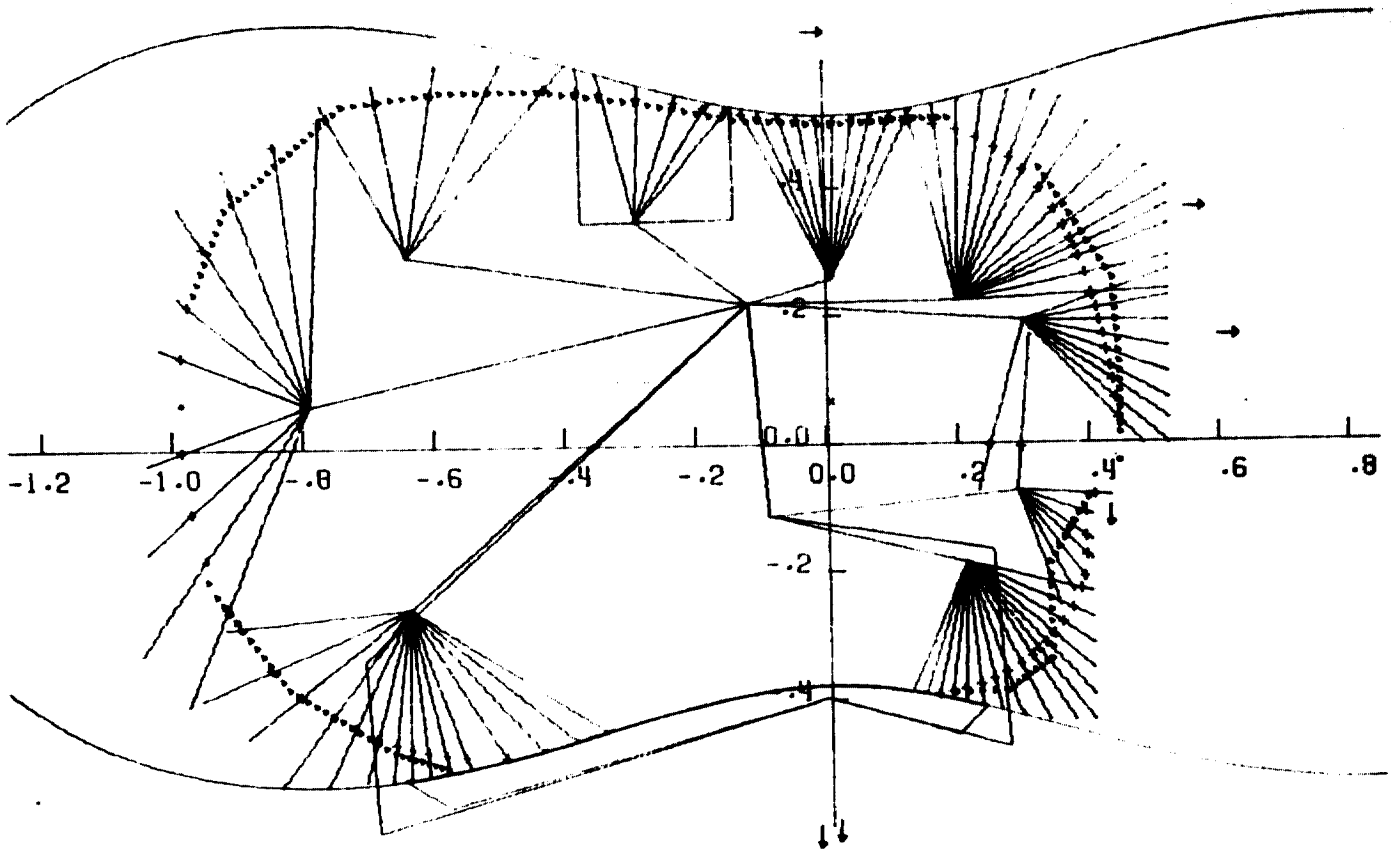

$M_\infty = 0.682$ $C_\ell = 0.400$ $t/c = 0.208$

(b) A hodograph plane.

Figure 1.- Continued.

TAPE 6, PATH 0

2	0	
-.800	0.000	2
-1.000	0.000	2
2	0	
.300	0.000	2
.440	-.100	2

TAPE 7

-6	-14	4	-.12	.22	.08	1.40	.682	-.007	-.067	.105	1.50	3			
19	1	2	5	6	45	46	13	14	41	42	49	50	53	54	57
58	61	62	34												

-.279	-.465	.600	.170	.013	-.157	.550	.370
0.000	0.000	0.000	0.000	-.086	-.220	-.030	.650
0.000	0.000	0.000	0.000	0.000	0.000	0.000	0.000
0.000	0.000	0.000	0.000	0.000	0.000	0.000	0.000
0.000	.025	0.000	-.600	0.000	0.000	0.000	0.000
.071	.033	-.030	-.610	-.039	.080	.420	-.110
.033	-.084	.200	.010	.129	-.258	-.100	.050
.177	-.054	.246	-.001	.030	-.013	1.000	1.000

(c) Tape 6 and tape 7 input parameters.

Figure 1.- Continued.

AUTOMATION PATHS

```
4   0
 -.960   -.280  -2
 -.840   -.440   1
 -.680   -.540   1
 -.600   -.565   1

4   0
 -.800   0.000   2
 -.980    .180  -2
 -.930    .310   1
 -.750    .470   1

5   0
 -.150    .440  -1
 -.300    .470   1
 -.450    .490   1
 -.600    .490   1
 -.750    .470   1

4   0
 -.150    .440  -1
 0.000    .430   1
  .130    .440   1
  .180    .440   1

5   0
  .320    .360  -1
  .430    .190   1
  .440    .060   1
  .440   0.000   1
  .440   -.050   1

6   0
 -.093   -.240   2
  .180   -.450   1
  .260   -.450   1
  .330   -.400   1
  .330   -.250   1
  .390   -.150   1
```

(d) Automation path inputs.

Figure 1.- Concluded.

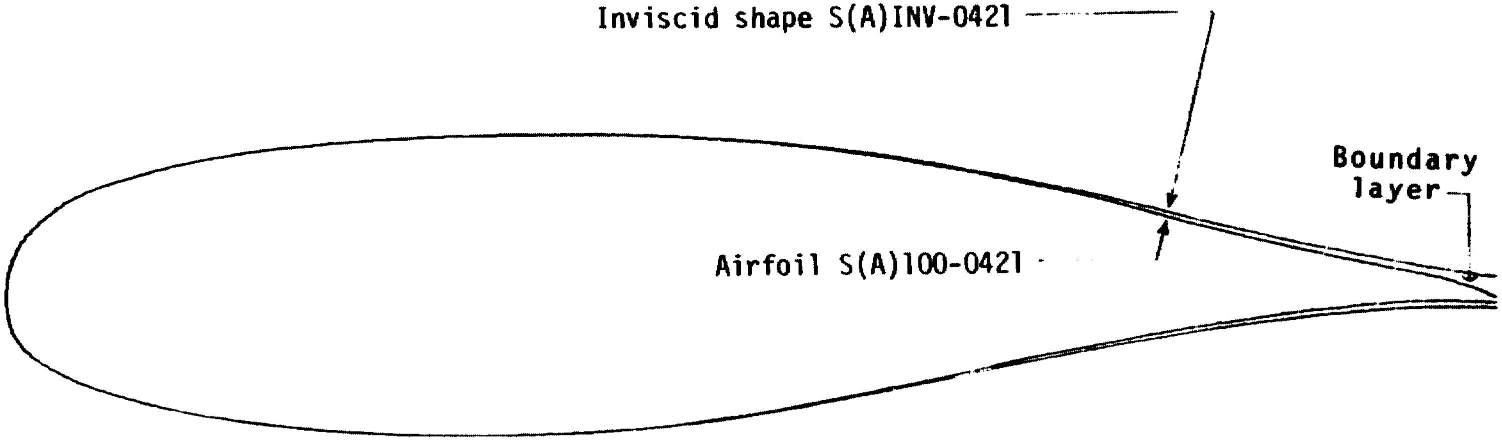

(a) Airfoil for N_R = 100 million.

Figure 2.- Inviscid shape and two corresponding airfoils.

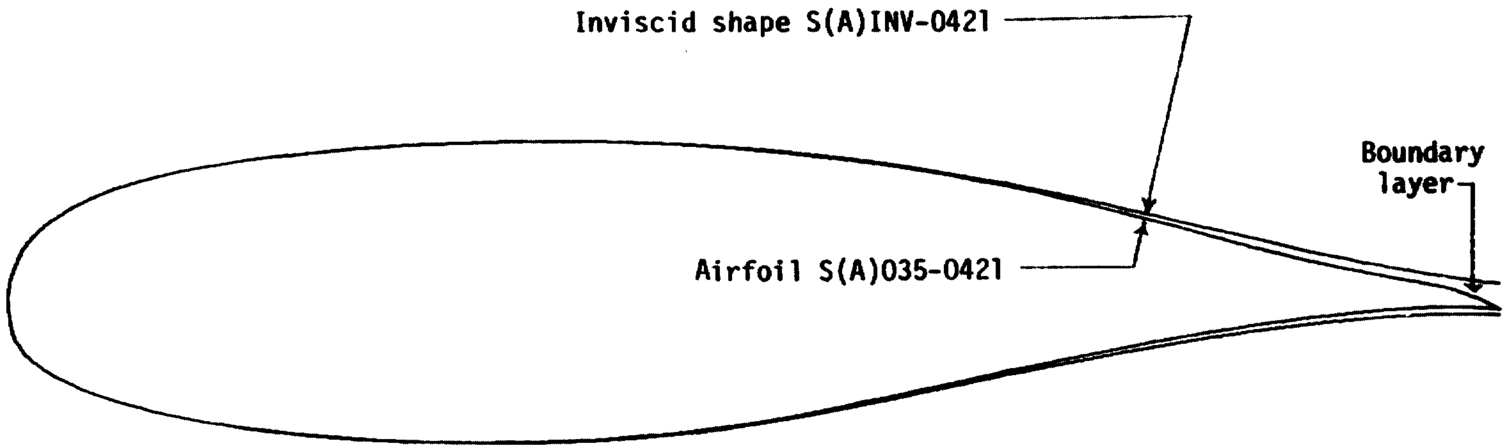

(b) Airfoil for N_R = 35 million.

Figure 2.- Concluded.

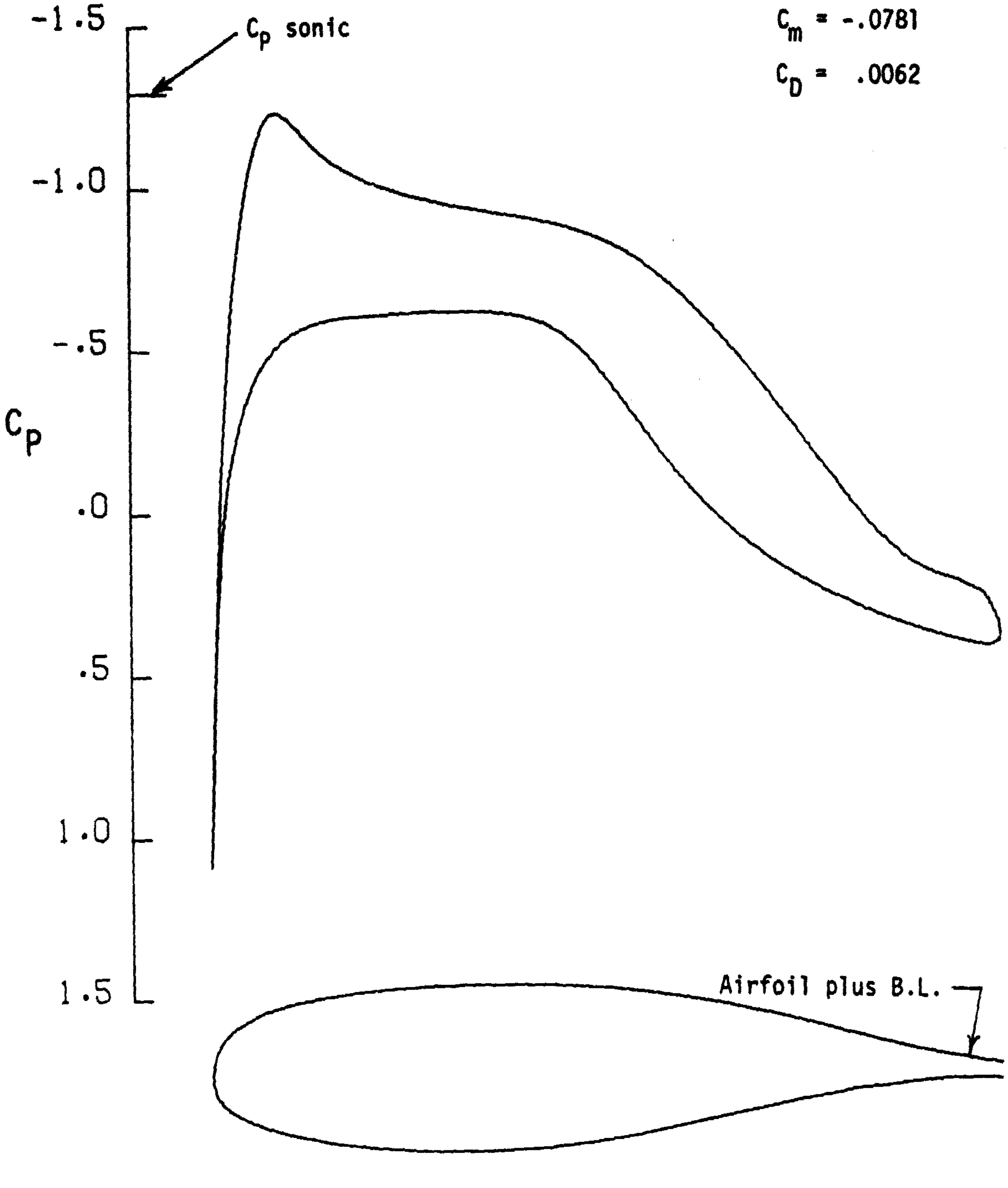

(a) $M_\infty = 0.60$.

Figure 3.- Analysis of airfoil S(A)100-0421 at the design Reynolds number and lift coefficient (N_R = 100 million and $C_\ell = 0.40$) for various Mach numbers.

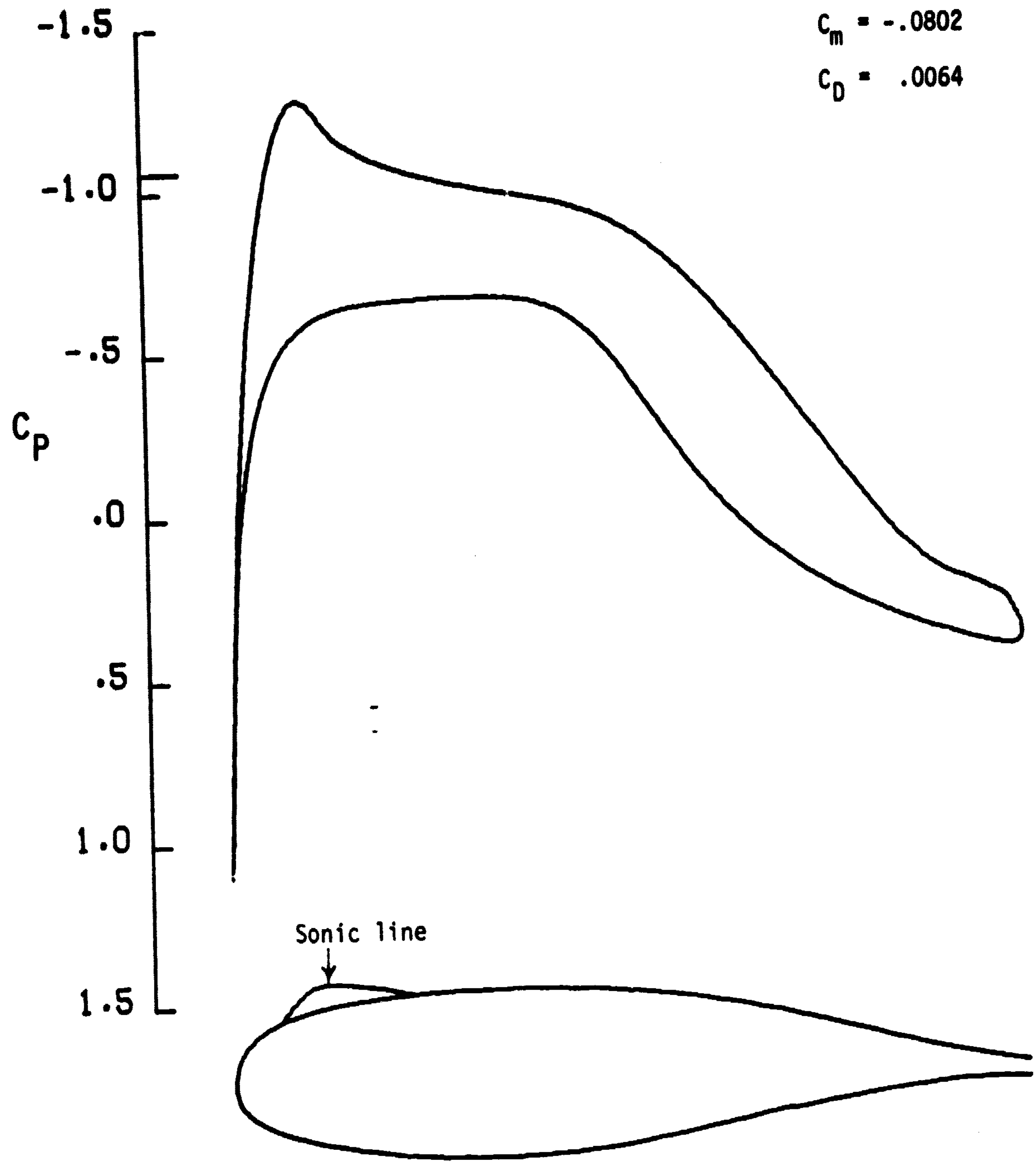

(b) M_∞ = 0.64.

Figure 3.- Continued.

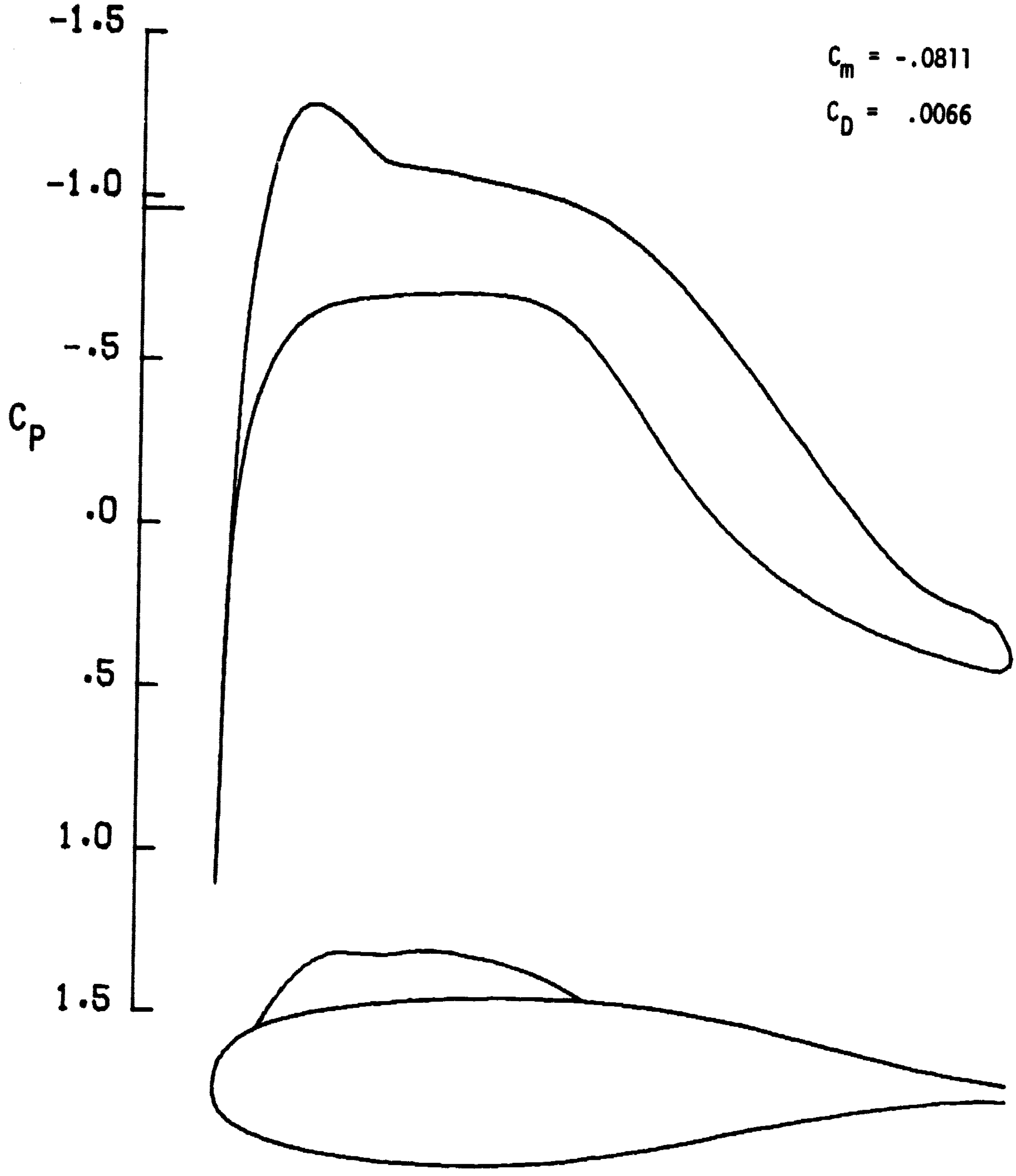

(c) M_∞ = 0.66.

Figure 3.- Continued.

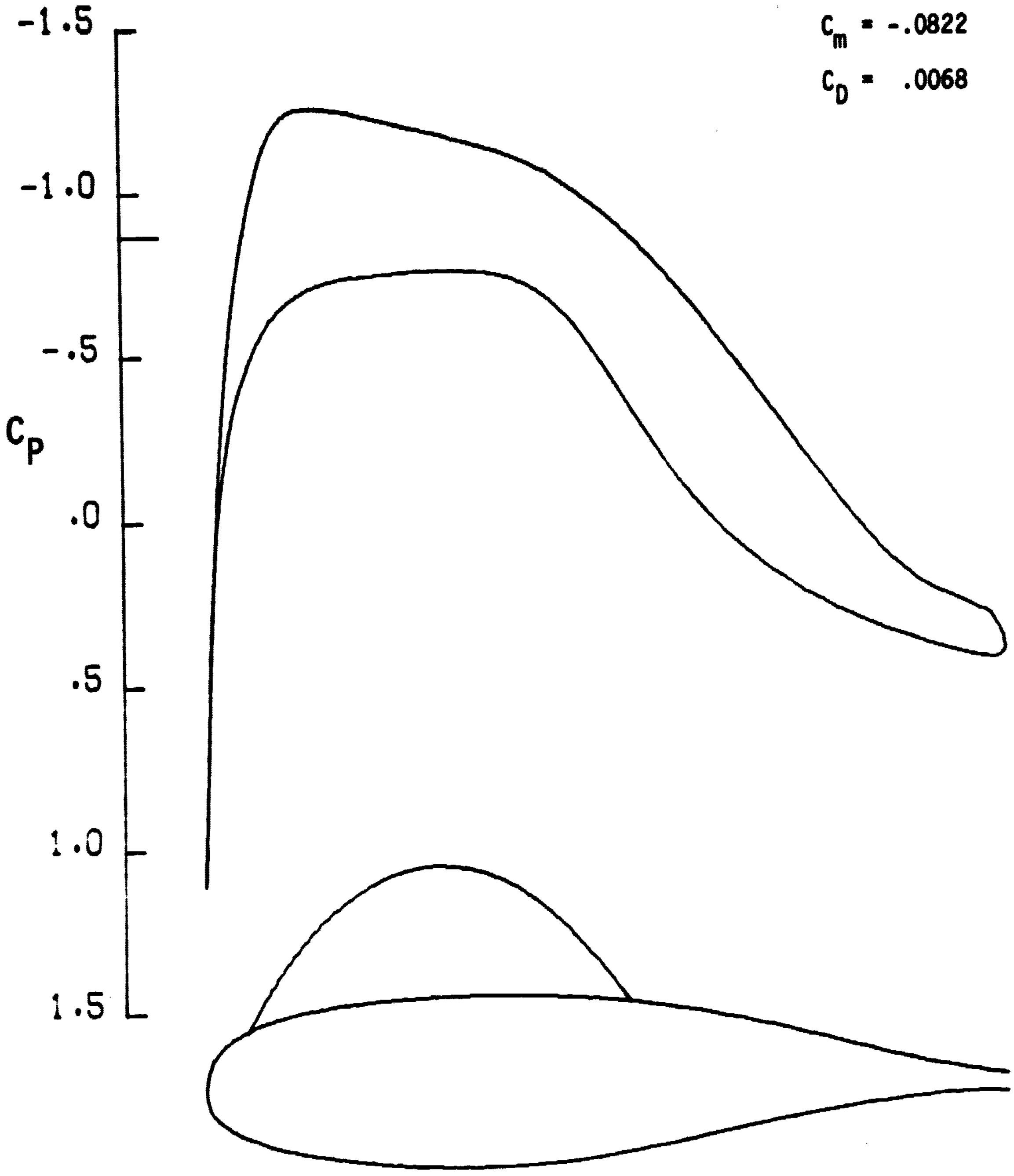

(d) Shockless design condition, M_∞ = 0.68.

Figure 3.- Continued.

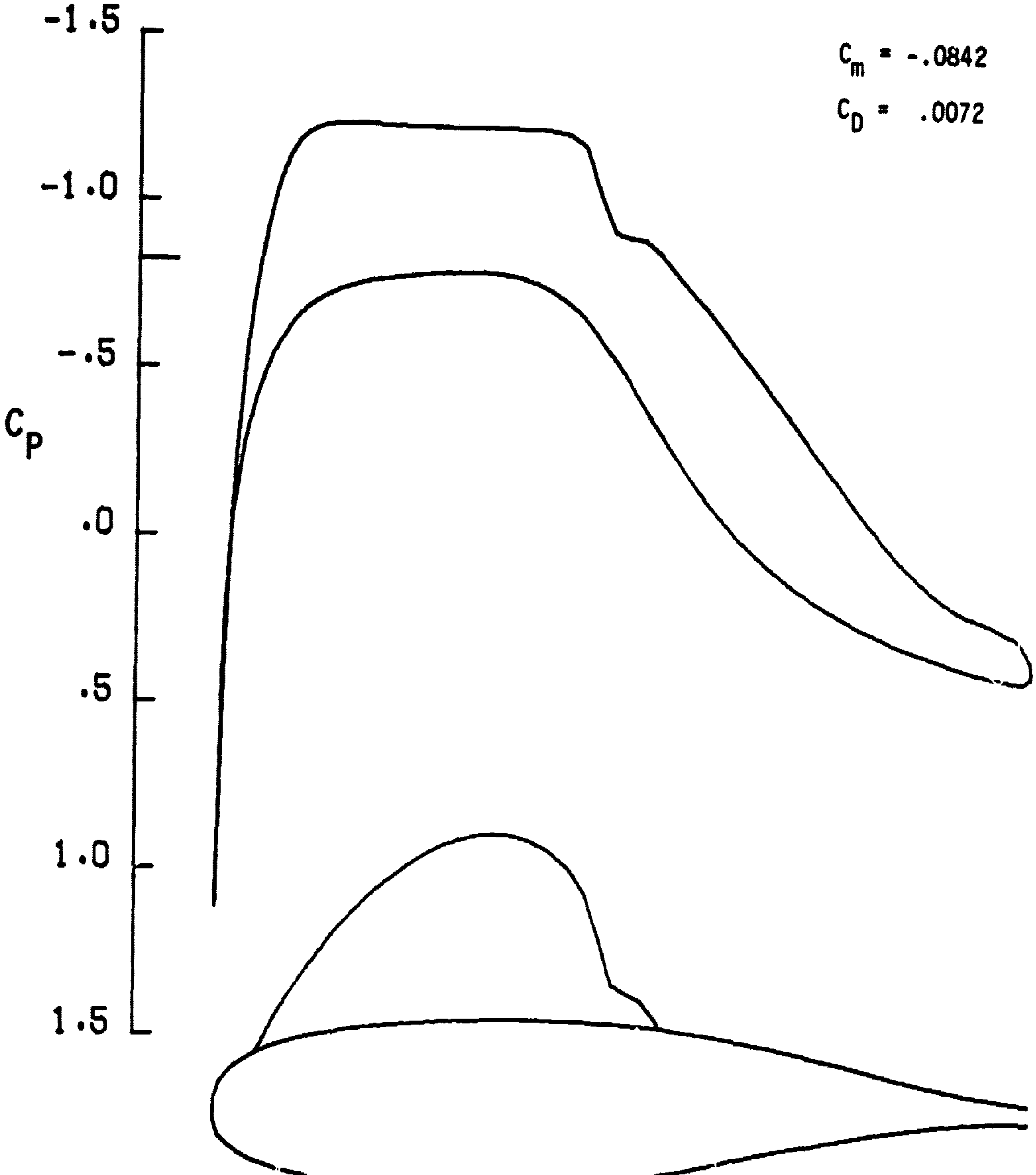

(e) M_∞ = 0.69.

Figure 3.- Continued.

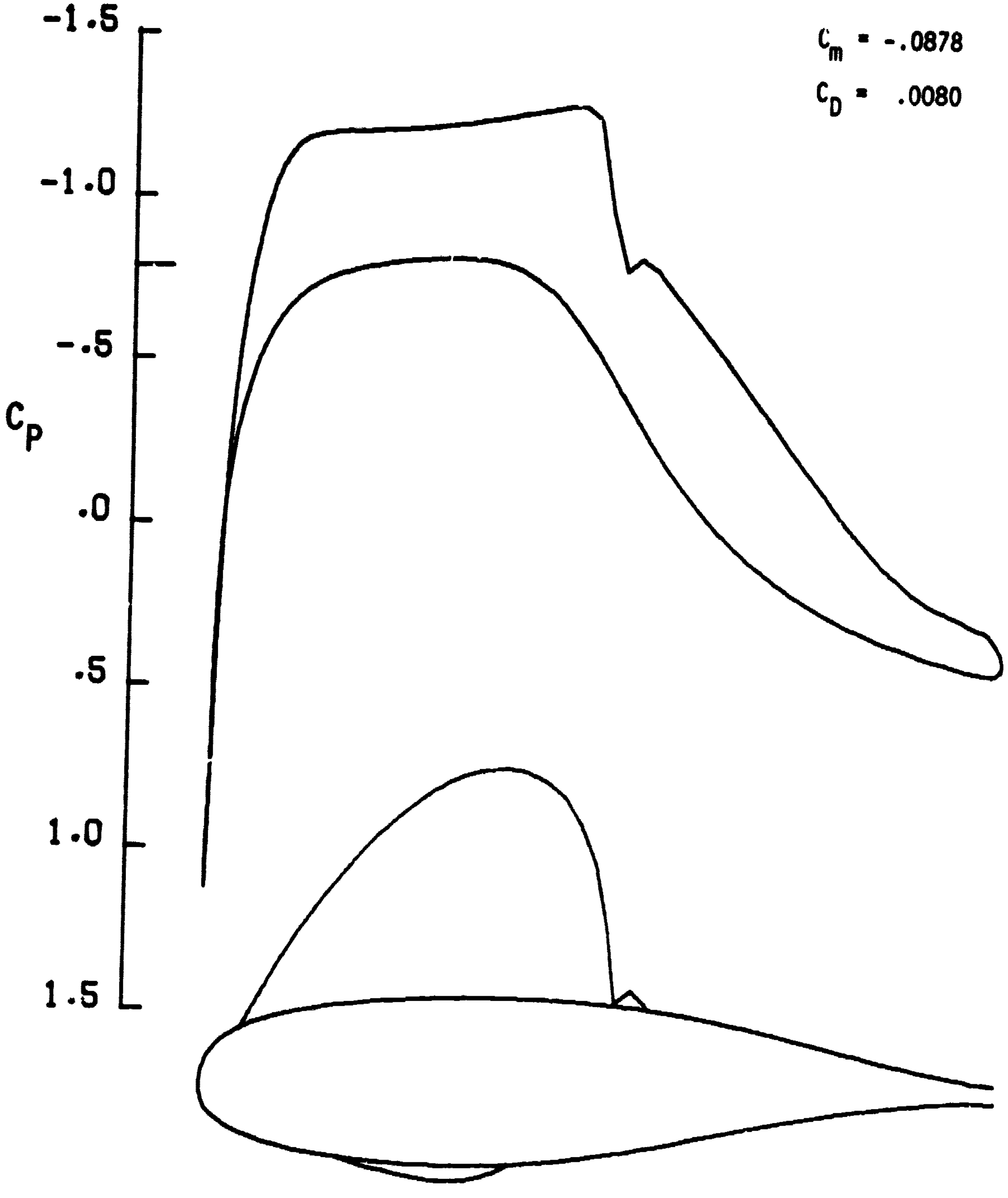

(f) M_∞ = 0.70.

Figure 3 - Concluded.

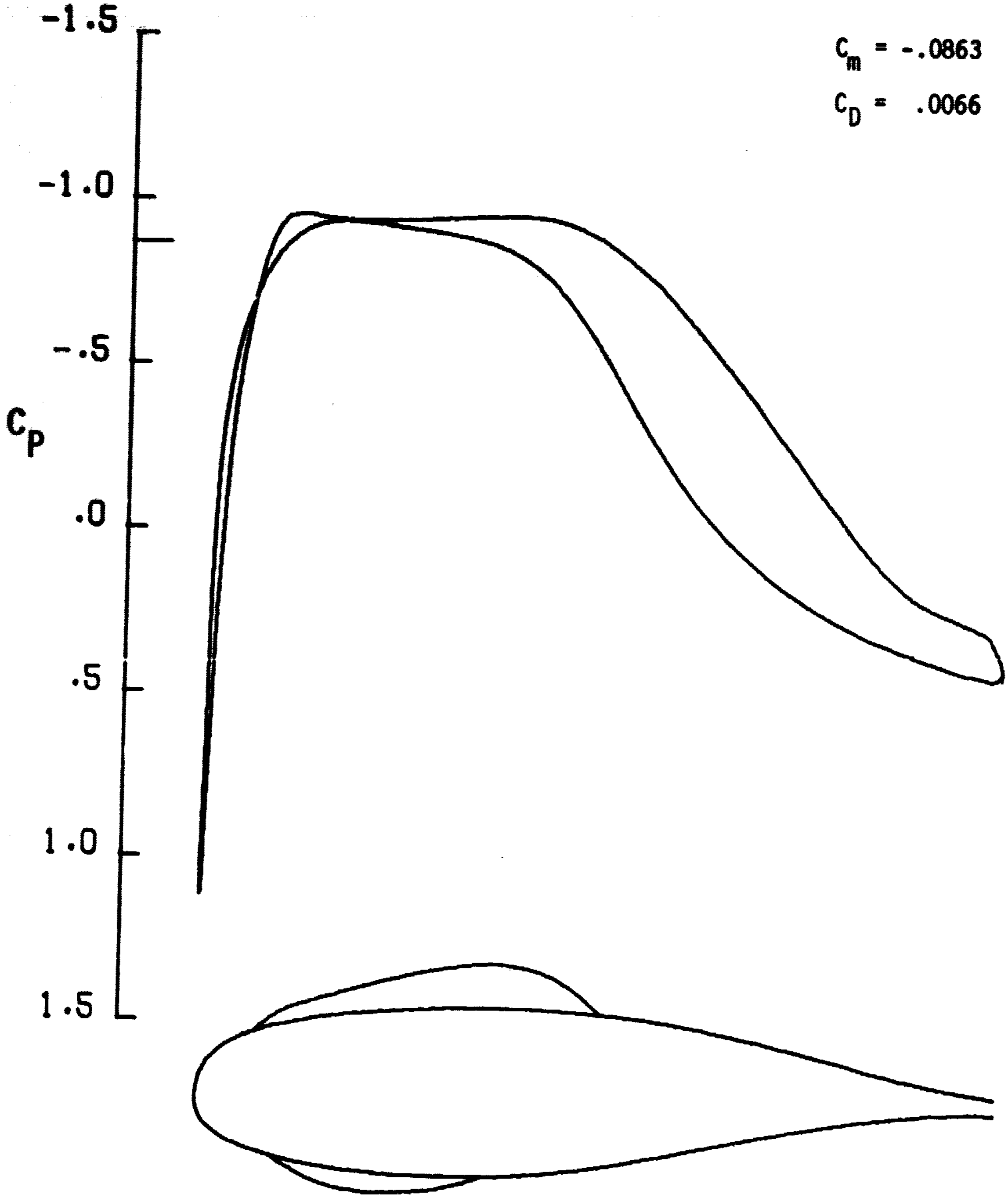

(a) $C_\ell = 0.20$.

Figure 4.- Analysis of airfoil S(A)100-0421 at the design Reynolds number and Mach number (N_R = 100 million and M_∞ = 0.68) for various lift coefficients.

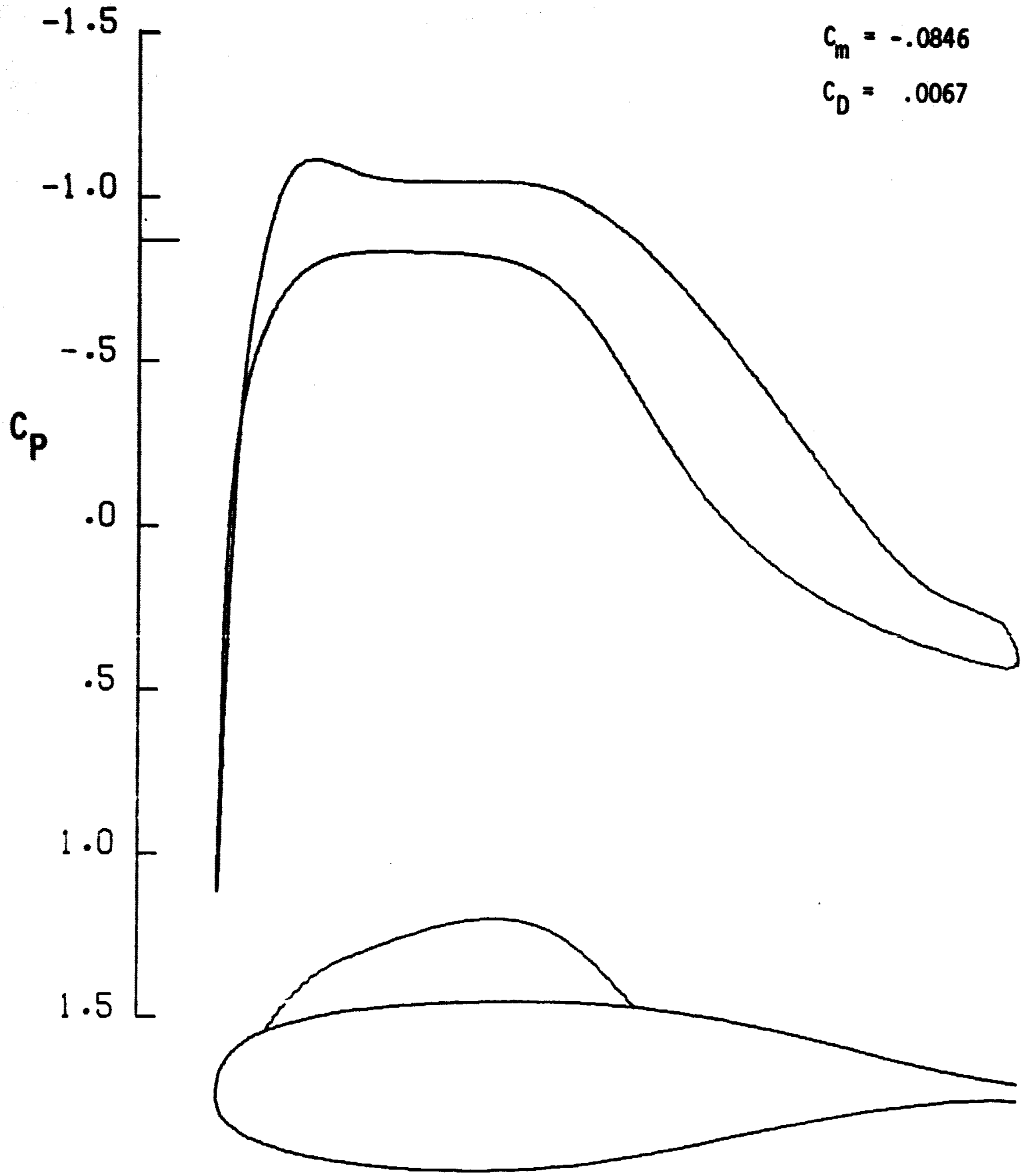

(b) $C_\ell = 0.30$.

Figure 4.- Continued.

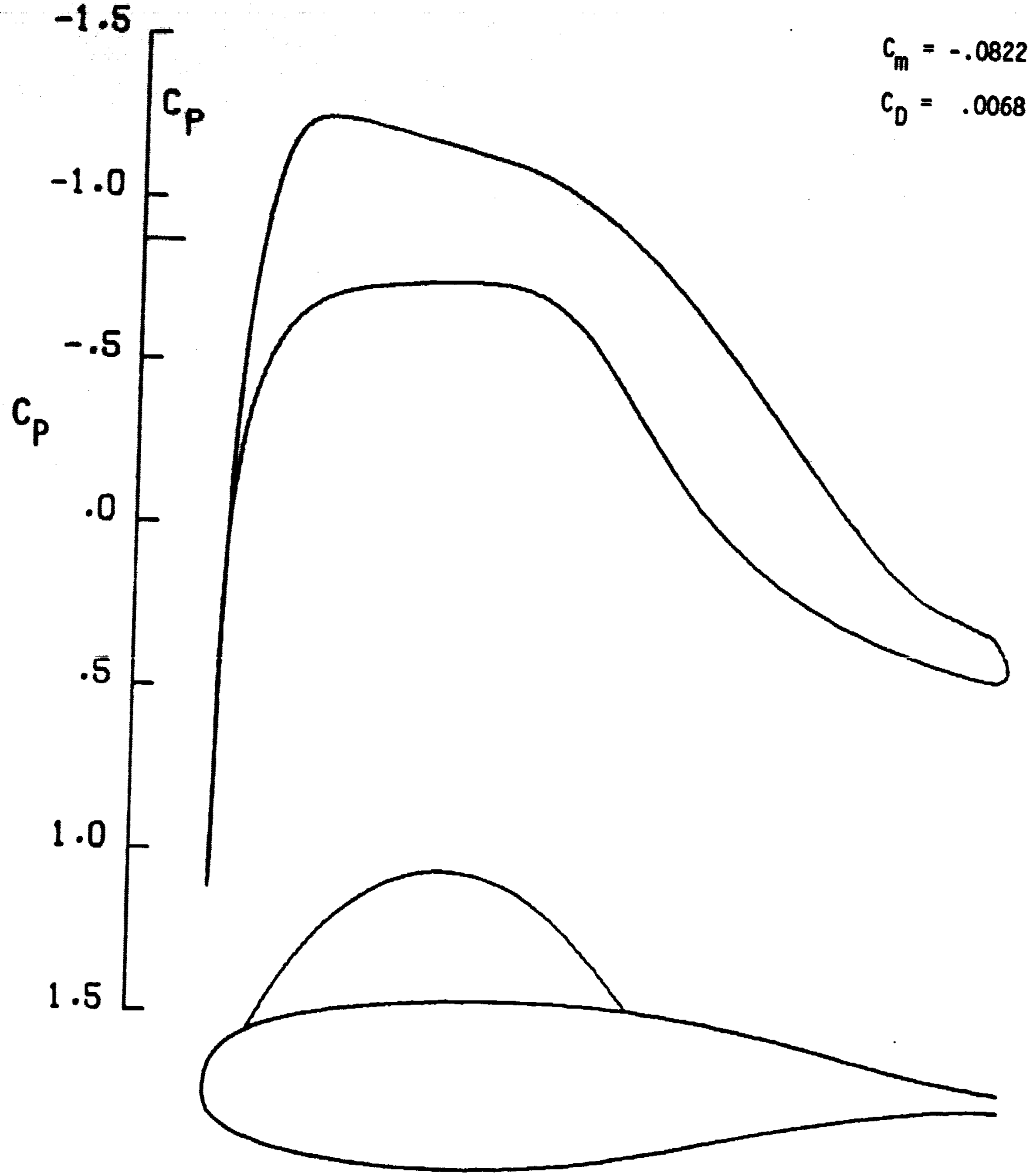

(c) Shockless design condition, C_ℓ = 0.40.

Figure 4.- Continued.

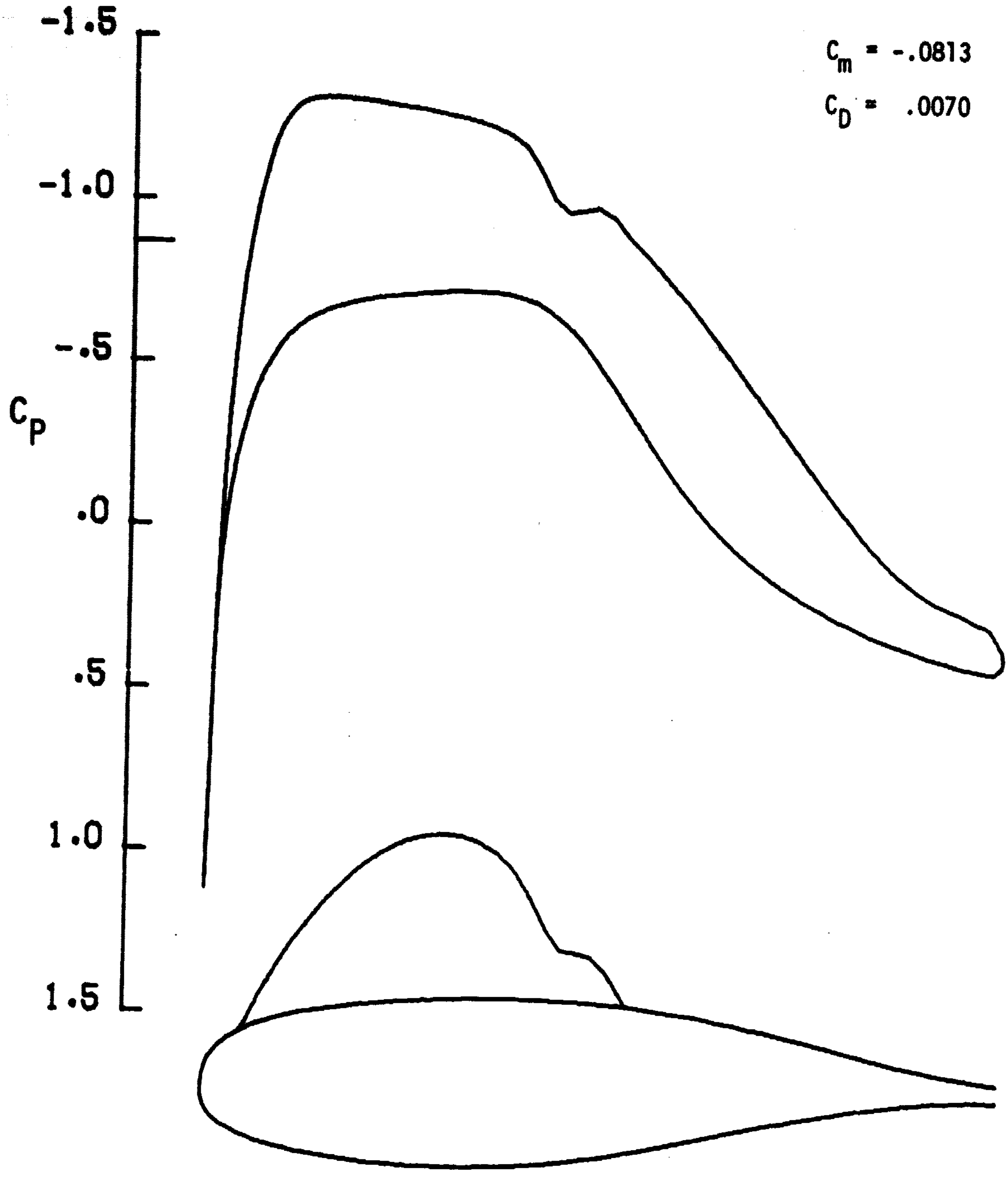

(d) C_ℓ = 0.45.

Figure 4.- Continued.

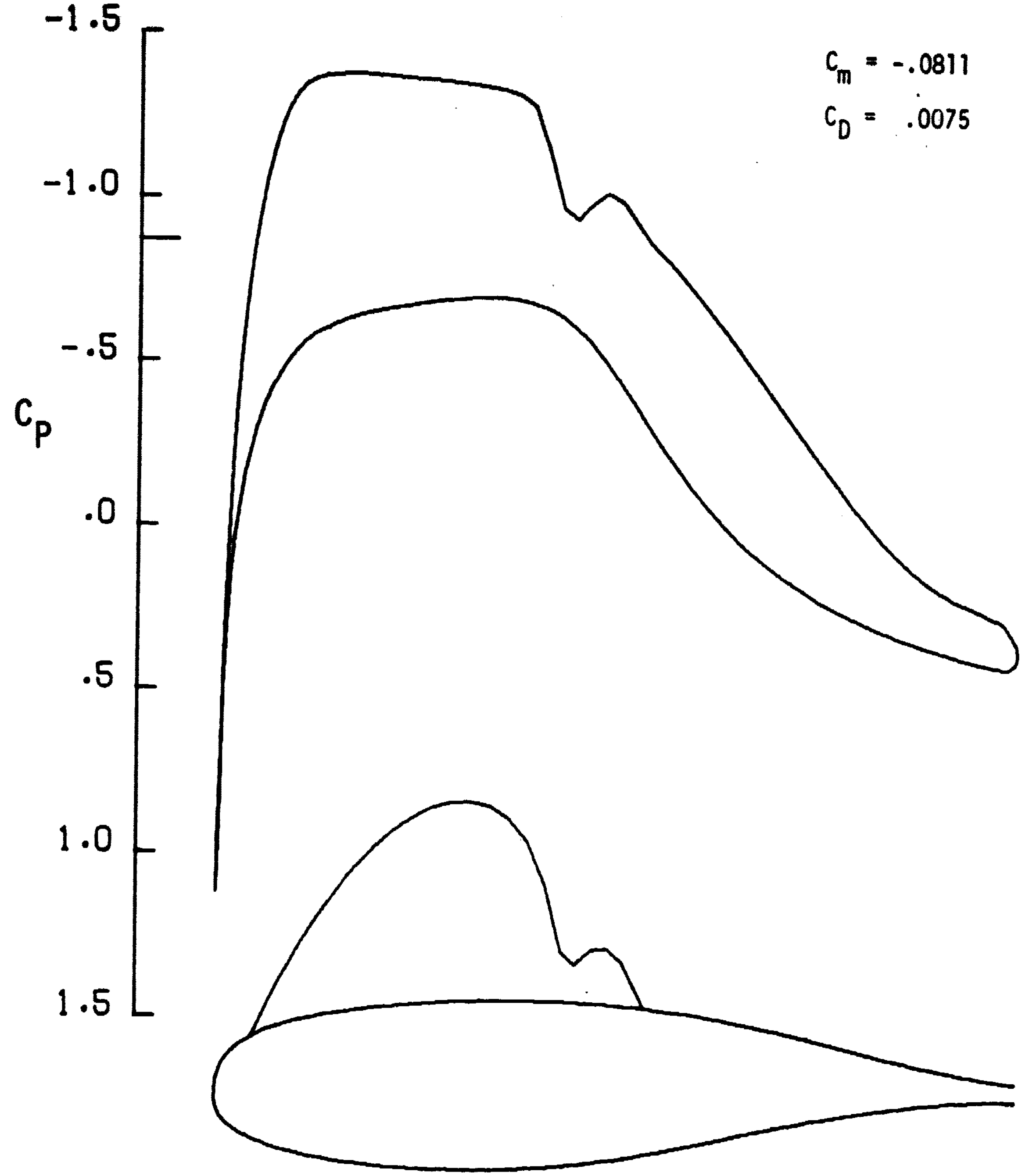

(e) C_ℓ = 0.50.

Figure 4.- Concluded.

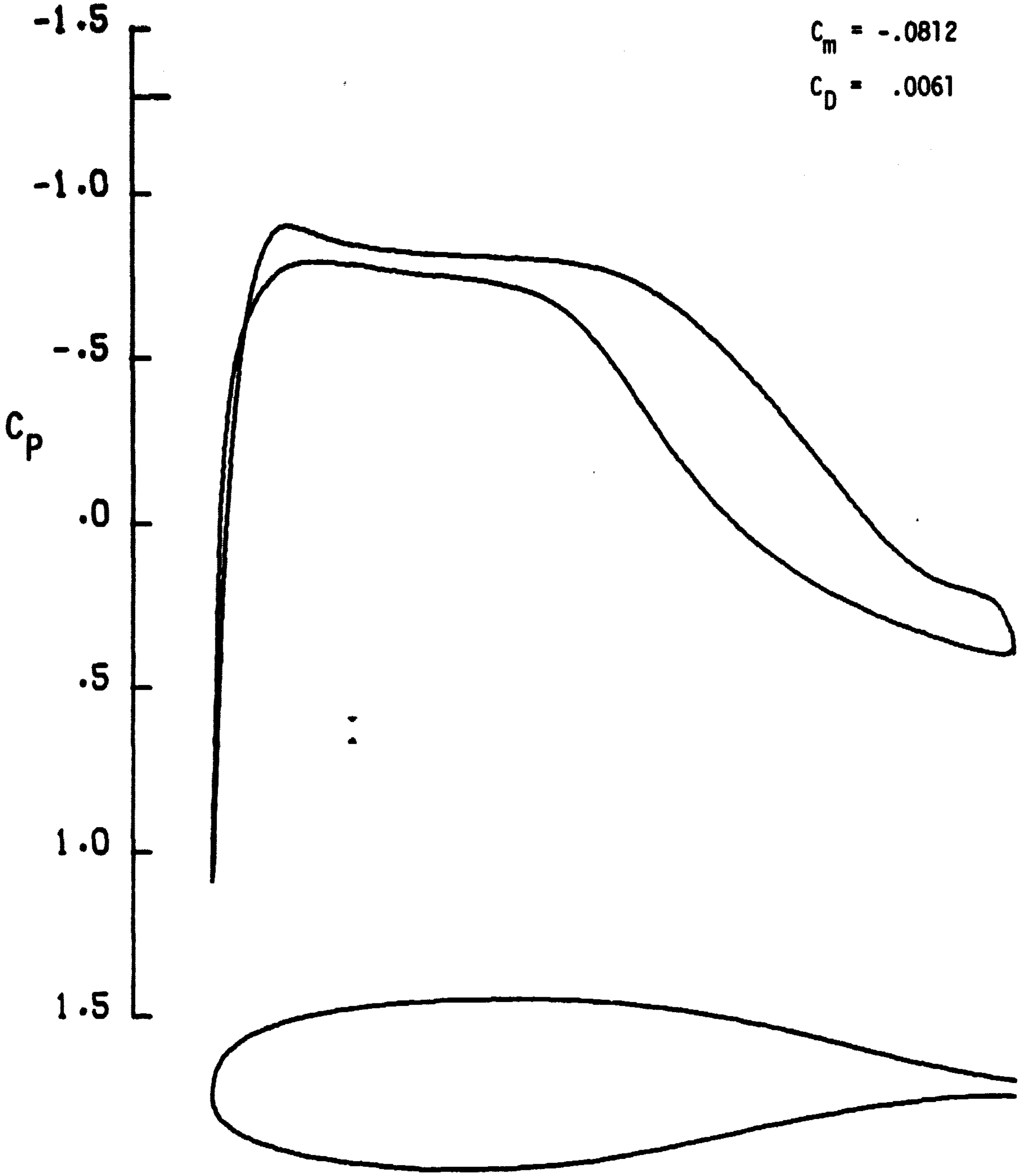

(a) $C_\ell = 0.20$.

Figure 5.- Analysis of airfoil S(A)100-0421 at the design Reynolds number (N_R = 100 million) and a Mach number of $M_\infty = 0.60$ for various lift coefficients.

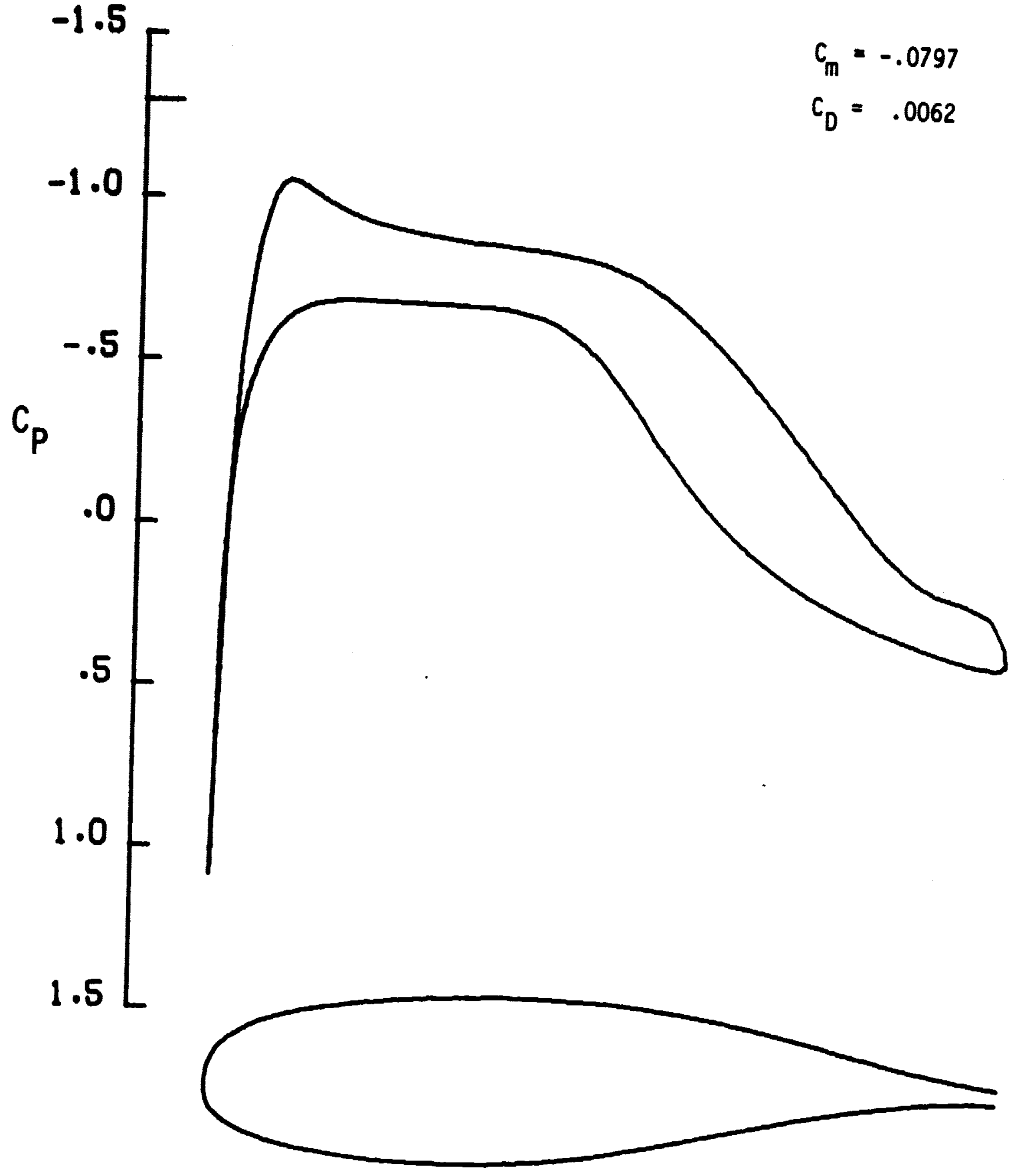

(b) C_ℓ = 0.30.

Figure 5.- Continued.

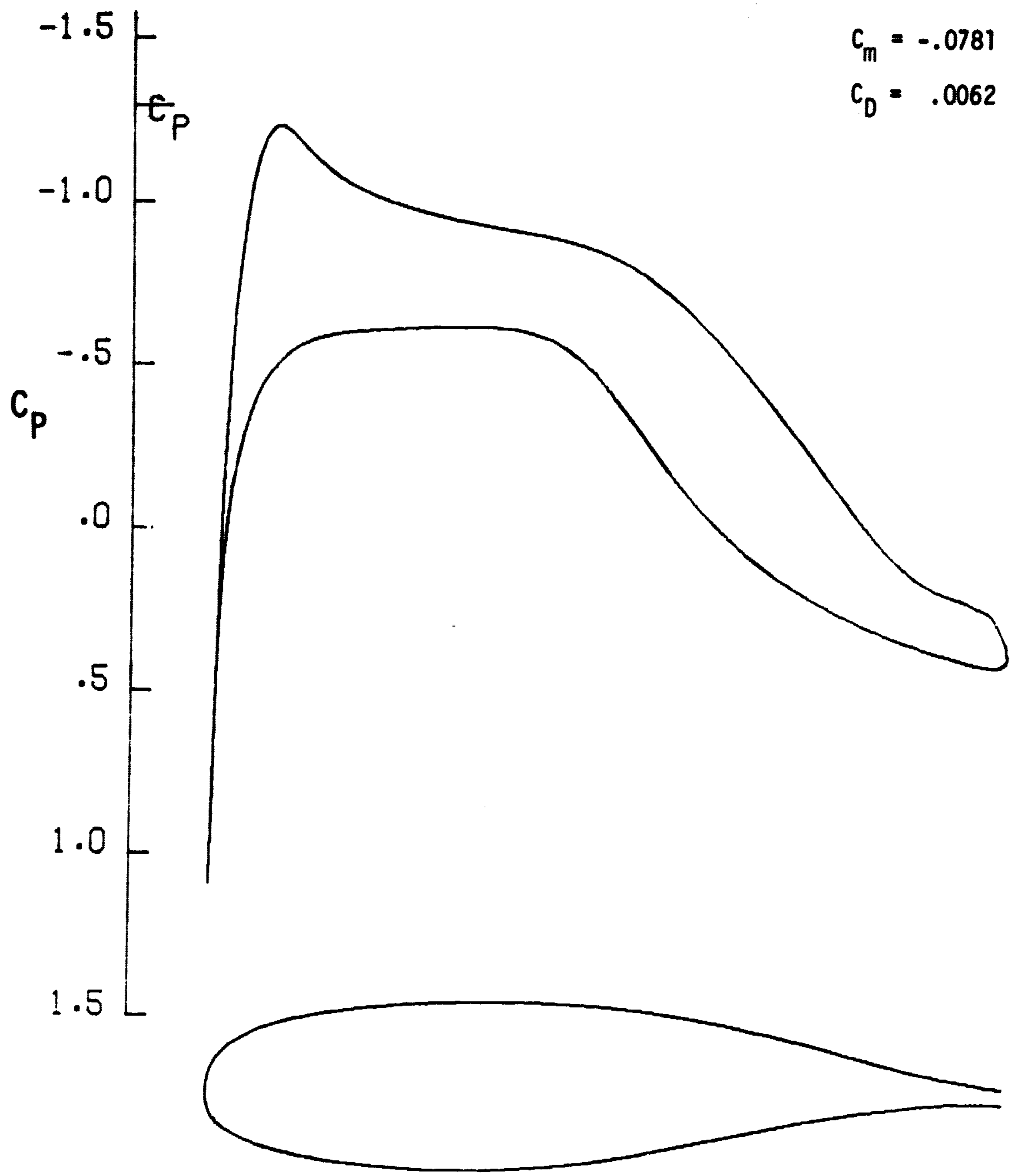

(c) C_ℓ = 0.40.

Figure 5.- Continued.

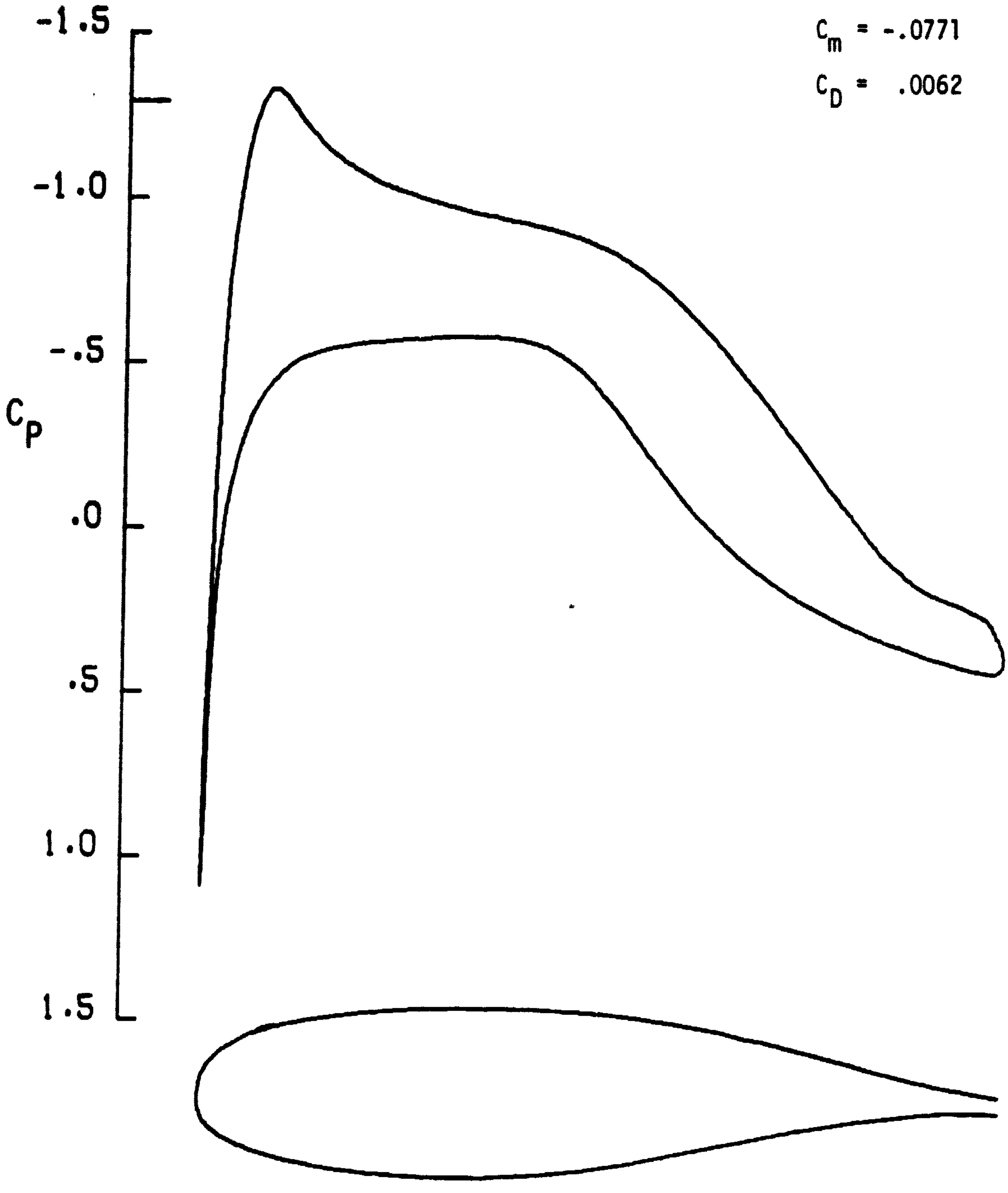

(d) C_ℓ = 0.45.

Figure 5.- Continued.

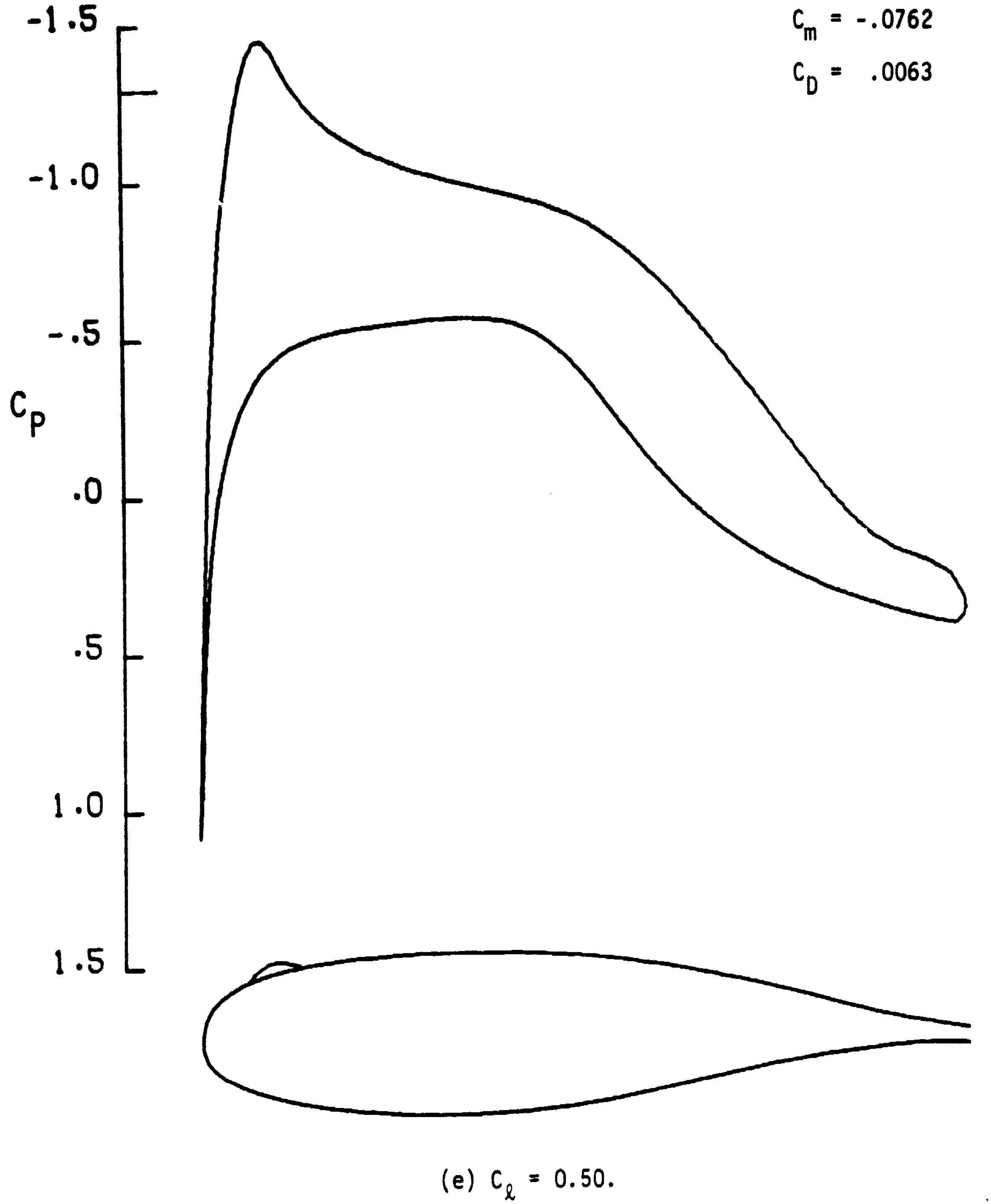

(e) C_ℓ = 0.50.

Figure 5.- Concluded.

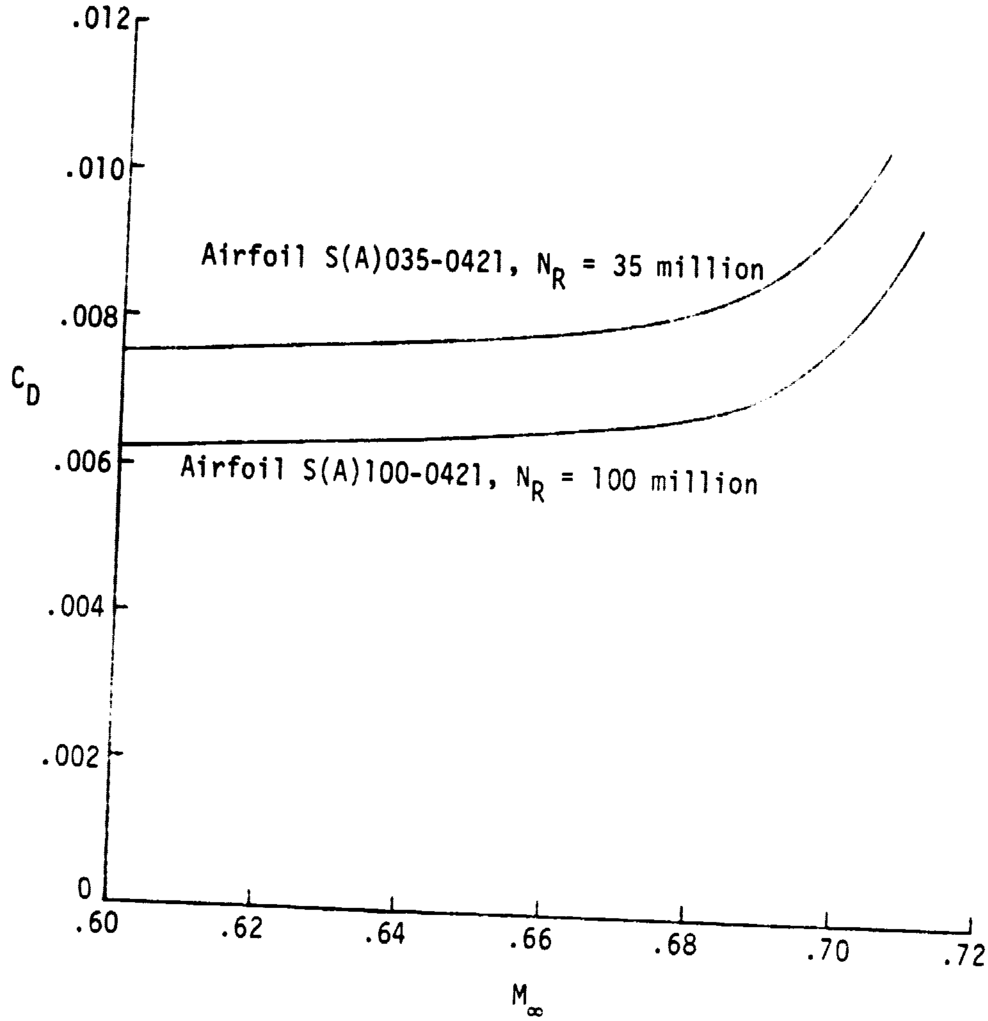

Figure 6.- Variation of drag coefficient with Mach number for the two airfoils at their design Reynolds numbers and C_ℓ = 0.40.